ASIAN JOURNAL OF CIVIL ENGINEERING (BHRC) VOL. 17, NO. 1 (2016)
PAGES 107-126

USING MORE ACCURATE STRAIN FOR THREE-DIMENSIONAL TRUSS ANALYSIS

M. Rezaiee-Pajand* and R. Naserian
Department of Civil Engineering, Ferdowsi University of Mashhad, Mashhad, Iran

Received: 18 June 2015; **Accepted:** 12 August 2015

ABSTRACT

Instead of the usual neglecting, this study takes advantage of the second-order axial strain terms in the elastic constitutive equation of three-dimensional truss. This leads to higher-order terms on the resulting unbalanced force and on its corresponding tangent stiffness. The finite element procedure and updated Lagrangian descriptions are utilized with the new stiffness matrix. Furthermore, governing equilibrium equations are solved by using cylindrical arc-length approach. The validity of the proposed algorithm is checked by numerical examples. The outcomes indicate that the authors' formulation possesses the ability to trace the equilibrium path completely. Moreover, the obtained answers are identical with the exact results of other researchers.

Keywords: Second-order strain; tangent stiffness matrix; space truss; updated Lagrangian; cylindrical arc-length.

1. INTRODUCTION

Nonlinear analysis is needed for reflecting the real behavior of some constructions. Indeed, most of the structures exhibit a number of inelastic behaviors before reaching their ultimate strength. There are two different types of nonlinear performance in the analysis of structures, which are called material and geometrical nonlinearity. The change of geometry under external loads is a critical criterion in the static position of space trusses. Many studies have been conducted into the nonlinear response of truss structures resulting from the changes in geometry of truss members. Jagannathan *et al.* and Rothert *et al.* concentrated on the behavior of snap-through buckling in reticulated truss structures [1, 2]. The stability analysis of lattice structures was performed by Holzer *et al.* [3]. Papadrakakis utilized vector iteration method for spatial structures [4], and dynamic relaxation procedure for truss structures [5]. As a general rule, the response of geometrical nonlinear structures under large loads has some limit points. In another study, the performances of snap-through and bifurcation points

*E-mail address of the corresponding author: rezaiee@um.ac.ir (M. Rezaiee-Pajand)

of a simple truss were explored by Pecknold *et al.* [6].

Researchers also introduced material nonlinearity in the real behavior of structures. The effect of local buckling on the overall response of geometrically perfect and imperfect truss structures was studied by Kondoh and Atluri [7]. Hill *et al.* suggested a truss pattern based on the appropriate stress-strain relationships [8]. This model traces the plastic post-buckling nonlinear behavior of space truss structures. The ability of this model was improved by using dynamic relaxation technique by Ramesh and Krishnamoorthy [9] and arc-length method by Blandford [10, 11]. Toklu minimized potential energy using an adaptive local search procedure [12]. Saffari *et al.* utilized a mathematical algorithm and a set of suitable assumptions in order to present the accurate behavior of space truss structures [13]. Hills' truss model [8] was extended to perform the geometric and material nonlinear analysis of the space trusses by Thai and Kim [14]. Zhou *et al.* analyzed pre-stressed space trusses with geometrically imperfect [15]. Higher-order stiffness matrix was formulated in the elastic large displacement analysis of plane trusses by Torkamani and Shieh [16].

To find nonlinear solution of a structural problem by the finite element method requires the related consistent tangent stiffness matrix. According to the literature review, low and higher-order stiffness matrices are available for analyzing the plane truss. In the authors' best knowledge, no stiffness of the space truss has been so far derived, which contains the first and second-order terms of the strain vector. In fact, most of the researchers neglected the second-order terms of the axial strain. This action affects the satisfaction of equilibrium equation, as well as the convergence speed of the solution process. The purpose of this study is the nonlinear analysis of three-dimensional trusses by formulating a new tangent stiffness matrix. Additionally, the verification of this procedure through various numerical examples is another part of this research.

2. A HIGHER-ORDER STIFFNESS MATRIX

In this article, a new higher-order stiffness matrix will be formulated to be used for the geometric nonlinear analysis of three-dimensional trusses. In the following subsections, all assumptions and details of formulation will be presented. Later, numerical experiences will confirm the performances of the authors' technique.

2.1 Assumptions

To solve the aforementioned problem more effectively, the following assumptions are made in the calculation process:

1. The members of structures are straight, and without any imperfection and residual stresses. Furthermore, the centroidal axis of cross section and the longitudinal axis of the member are located on the one line.
2. The nodes of truss are assumed to be hinged, and members resist only axial loads.
3. Deformations occur only in the plane of the truss structure, and local buckling is ignored.
4. The cross sections of the structural members always remain plane and with members' deformations, the cross sections remain normal to the longitudinal axes of the members.

It is reminded that in the geometric nonlinear analysis, the shape of structure is

characterized in three ways. In the total Lagrangian description, the initial configuration of the member is entered into analysis, and governing equations are based on the reference shape [17]. On the other hand, the last obtained position of element is used as the reference configuration in the updated Lagrangian technique [18]. Finally, in the corotational approach, the combinations of the infinitesimal deformations and also rigid body motions are utilized [19]. Considering the more accurate results of the updated Lagrangian description and its more efficiency compared to the total Lagrangian, the former is used in this research [20, 21].

2.2 Finite element formulation

Fig. 1 shows a space truss element with six degrees of freedom. The nodal displacement vector is defined as follows:

$$\{d\}^T = \{u_1, v_1, w_1, u_2, v_2, w_2\} \tag{1}$$

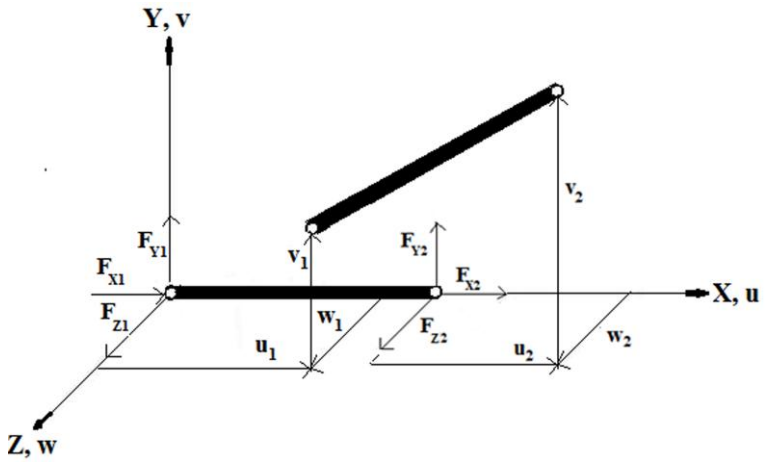

Figure 1. Local Coordinate system of a space truss element

Where, u_1, v_1, w_1 and u_2, v_2, w_2 are referred DOFs corresponding to the translations of nodes 1 and 2, along the directions of x, y and z, respectively. For presenting the displacement field, which determinates the motions of an arbitrary point in terms of the nodal displacements, the coming shape functions will be used:

$$u(x) = [N_u]\{d\} \tag{2}$$

$$v(x) = [N_v]\{d\} \tag{3}$$

$$w(x) = [N_w]\{d\} \tag{4}$$

In these equations, $[N_u]$, $[N_v]$ and $[N_w]$ are the shape functions for the axial and lateral displacements of a truss member with length of L. According to Fig. 1, the nodal force vector can be written in the below form:

$$\{f\}^T = \left\{F_{x1}, F_{y1}, F_{z1}, F_{x2}, F_{y2}, F_{z2}\right\} \tag{5}$$

Here, F_{x1}, F_{y1}, F_{z1} and F_{x2}, F_{y2}, F_{z2} are the components of force corresponding to nodes 1 and 2, along the directions of x, y and z, respectively.

As it is shown in Fig. 1, the next boundary conditions of a three-dimensional truss member are held:

$$\begin{cases} x = 0, & u = u_1 \ , \quad v = v_1 \ , \quad w = w_1 \\ \text{x = L}, & u = u_2 \ , \quad v = v_2 \ , \quad w = w_2 \end{cases} \tag{6}$$

Using the boundary conditions of equation (6), the vector of shape functions can be presented in the following form:

$$[N_u] = \left[1 - \frac{x}{L}, 0, 0, \frac{x}{L}, 0, 0\right] \tag{7}$$

$$[N_v] = \left[0, 1 - \frac{x}{L}, 0, 0, \frac{x}{L}, 0\right] \tag{8}$$

$$[N_w] = \left[0, 0, 1 - \frac{x}{L}, 0, 0, \frac{x}{L}\right] \tag{9}$$

2.3 Equilibrium equations

It is assumed that no permanent strain is retained when unloading accrues, and structure has nonlinear elastic behavior. In this circumstance, the incremental equilibrium equation can be derived by minimizing total potential energy and utilizing the virtual work principle. Therefore, the following relation is held:

$$\delta(\Delta\Pi) = \delta(\Delta U) - \delta(\Delta W) = 0 \tag{10}$$

Where, U is the strain energy, and W is the potential work of the member applied force. In addition, σ and ε are axial stress and strain, respectively. The axial stress of the member is defined as:

$$\delta(\Delta U) = \delta\left(\int_v \sigma \, d\varepsilon \, dv\right) \tag{11}$$

$$\delta(\Delta W) = \{\delta d\}^T \{f\} \tag{12}$$

$$\sigma = \sigma_0 + E\,\varepsilon \tag{13}$$

In this equation, σ_0 is the axial stress in the reference configuration, and E is the modulus of elasticity. The axial strain of the truss member can be decomposed into two following parts of linear and nonlinear one [22]:

$$\varepsilon_{xx} = e_{xx} + \mu_{xx} \tag{14}$$

Where, e_{xx} is the linear part and μ_{xx} is the nonlinear portion of strain. By replacing equations (11-14) into relationship (10), the incremental static equation can be expressed as below:

$$\begin{aligned}\delta(\Delta\Pi) = &\int_v E e_{xx}\delta e_{xx}dv + \int_v E\mu_{xx}\delta e_{xx}dv + \int_v E e_{xx}\delta\mu_{xx}dv + \\ &\int_v E\mu_{xx}\delta\mu_{xx}dv + \int_v \sigma_0\delta e_{xx}dv + \int_v \sigma_0\delta\mu_{xx}dv - \{\delta d\}^T\{f\} = 0\end{aligned} \tag{15}$$

The subsequent linear and nonlinear expressions of strain will be obtained by employing equations (2- 4):

$$e_{xx} = \frac{du}{dx} = [N'_u]\{d\} \tag{16}$$

$$\begin{aligned}2\mu_{xx} = &(\frac{du}{dx})^2 + (\frac{dv}{dx})^2 + (\frac{dw}{dx})^2 = \{d\}^T[N'_u]^T[N'_u]\{d\} + \\ &\{d\}^T[N'_v]^T[N'_v]\{d\} + \{d\}^T[N'_w]^T[N'_w]\{d\}\end{aligned} \tag{17}$$

The following relations give the first variation of the linear and nonlinear strain:

$$\delta e_{xx} = \{\delta d\}^T[N'_u] \tag{18}$$

$$\begin{aligned}\delta\mu_{xx} = &\{\delta d\}^T[N'_u]^T[N'_u]\{d\} + \{\delta d\}^T[N'_v]^T[N'_v]\{d\} + \\ &\{\delta d\}^T[N'_w]^T[N'_w]\{d\}\end{aligned} \tag{19}$$

$$[N'] = \frac{dN}{dx} \tag{20}$$

In the last equality, [N'] is the derivative of shape functions with respect to x parameter. Finally, by applying equations (16-19), the incremental equilibrium relation (15) will be changed to below shape:

$$\begin{aligned}&\delta(\Delta\Pi) = \{\delta d\}^T\int_v E[N'_u]^T[N'_u]\{d\}dv + \{\delta d\}^T\int_v \frac{E}{2}[N'_u]^T(\{d\}^T[N'_u]^T[N'_u] + \\ &\{d\}^T[N'_v]^T[N'_v] + \{d\}^T[N'_w]^T[N'_w])\{d\}dv + \{\delta d\}^T\int_v E([N'_u]^T[N'_u] + [N'_v]^T[N'_v] + \\ &[N'_w]^T[N'_w])\{d\}[N'_u]\{d\}dv + \{\delta d\}^T\int_v \frac{E}{2}([N'_u]^T[N'_u] + [N'_v]^T[N'_v] + [N'_w]^T[N'_w])\{d\}\{d\}^T \\ &([N'_u]^T[N'_u] + [N'_v]^T[N'_v] + [N'_w]^T[N'_w])\{d\}dv + \{\delta d\}^T\int_v \sigma_0[N'_u]^T dv + \\ &\{\delta d\}^T\int_v \sigma_0([N'_u]^T[N'_u] + [N'_v]^T[N'_v] + [N'_w]^T[N'_w])\{d\}dv - \{\delta d\}^T\{f\} = 0\end{aligned} \tag{21}$$

2.4 Component of the stiffness matrix

The incremental static equation (21) can be written as follows:

$$\delta(\Delta\Gamma) = \{\delta d\}^T [K]\{d\} - \{\delta d\}^T \{f\} = 0 \tag{22}$$

Using relation (22), the higher-order stiffness matrix of the space truss member is obtained in the below form:

$$[K_L] = [K_0] + [K_p] + [K_1] + [K_2] + [K_3] \tag{23}$$

$$[K_0] = \int_l EA[N'_u]^T [N'_u] dx \tag{24}$$

$$[K_p] = P\int_l ([N'_u]^T [N'_u] + [N'_v]^T [N'_v] + [N'_w]^T [N'_w]) dx \tag{25}$$

$$[K_1] = \frac{EA}{2}\int_l [N'_u]^T (\{d\}^T [N'_u]^T [N'_u] + \{d\}^T [N'_v]^T [N'_v] + \{d\}^T [N'_w]^T [N'_w]) dx \tag{26}$$

$$[K_2] = EA\int_l ([N'_u]^T [N'_u] + [N'_v]^T [N'_v] + [N'_w]^T [N'_w])(\{d\}[N'_u]) dx \tag{27}$$

$$[K_3] = \frac{EA}{2}\int_l ([N'_u]^T [N'_u] + [N'_v]^T [N'_v] + [N'_w]^T [N'_w])\{d\} \{d\}^T ([N'_u]^T [N'_u] + [N'_v]^T [N'_v] + [N'_w]^T [N'_w]) dx \tag{28}$$

$$\int_A dA = A, \quad \int_A \sigma_0 dA = P \tag{29}$$

The following parameters are employed in these formulas. Axial force is denoted by P. The member stiffness matrix of the space truss $[K_L]$ consists of five parts. The first item, $[K_0]$, is the elastic stiffness one. It is a constant division and is dependent on the linear behavior of structure. The second portion, $[K_P]$, is the geometric stiffness matrix of the member and is related to the axial force P at the beginning of each incremental step. Three other pieces, $[K_1]$, $[K_2]$ and $[K_3]$, are the higher-order stiffness matrices of the member. It should be added that the linear expressions of the incremental displacements of the member are included in the fractions $[K_1]$ and $[K_2]$. On the other hand, the $[K_3]$ matrix is written in terms of second degree functions of the member nodal motions. All of entries of the stiffness matrix $[K_L]$ are presented in the article appendix.

2.4.1 Rigid body test

To investigate the quality of the presented formulation, all the convergence criteria should be checked. The constant strain conditions, rigid body capabilities, element compatibility, and stability conditions can be verified by the patch test [23, 24]. On the other hand, since the patch test verifies merely the satisfaction of the basic differential equations and the

approximation in boundary conditions, it serves purely as a necessary condition for convergence.

Another technique is the eigenvalue test that can detect the instability, lack of invariance, and other flaws of a single element. These are the requirements by which the quality of competing elements can be estimated [25]. In other words, the eigenvalue test is one of the most widely used procedures for checking the element quality. It is important to note that the applications of the patch and eigenvalue methods are restricted to linear problems, in which the finite element is without the initial stresses or nodal forces. In a geometrically nonlinear analysis, the finite element will typically be deformed and acted upon by a set of nodal forces that are in equilibrium at the beginning of each incremental step. Having these nodal loads, a few iterations are performed at each step to ensure equilibrium of the structure. Obviously, the patch and eigenvalue tests, which have been devised for elements with no initial forces, cannot be directly applied to the nonlinear problems.

Therefore, the rigid body test is very useful in the nonlinear problems. To examine the quality of a nonlinear finite element, one cannot rely on the geometric stiffness matrix alone, but must consider the incremental stiffness equation as a whole to see if the new formulated element can really cope with the rigid body motion [26]. In this article, the correctness of the finite elements is examined by using rigid body test. The space truss element is rotated about its left end as a rigid body for 90 centigrade counterclockwise relative to the z axis. For this case, the nodal displacement vector is expressed as below:

$$\{d\}^T = \{0,0,0,-L,L,0\} \tag{30}$$

As a result, the following relationships are held:

$$\begin{aligned} \Delta u &= u_2 - u_1 = -L \\ \Delta v &= v_2 - v_1 = L \\ \Delta w &= w_2 - w_1 = 0 \end{aligned} \tag{31}$$

If multiplying equation (23) by the nodal displacement vector of equation (30), it is observed that the forces generated by the matrices $[K_0]$ and $[K_1]$ balance each other during this rigid body rotation. In a similar manner, the forces produced by the matrix $[K_2]$ balance those created by the matrix $[K_3]$ when subjected to this rigid body motion. It should be noted, these relations remain valid by ignoring the magnitude of the angle of rotation. On the other side of the considering equality, by adding the forces created by matrix $[K_P]$ to the initial forces of element, it is observed the axial force P will be rotated following the rigid body rotation. From the above three effects, the initial force P has been directed along the rotated axis of the space truss member, while its magnitude remains constant. It implies that the equilibrium of the member is kept after the rigid body motion. These results clearly demonstrate that the nonlinear stiffness matrices obtained in this research pass the rigid body test.

2.4.2 Transformation matrix

So far, the stiffness matrix of the equation (23) is calculated in the local coordinate of the member. A transformation medium is employed for converting the stiffness matrix to the global coordinate. The following relation shows how the stiffness matrix is changed from local coordinate to the global one:

$$[K_g] = [T]^T [K_L][T] \tag{32}$$

In the former equality, $[K_g]$ is the member stiffness matrix in the global coordinate, and matrix [T] is the transformation medium. This matrix converts the member stiffness from local coordinate to the global one. It should be noted that the total nonlinear stiffness matrix of the structure is obtained by assembling the incremental stiffness matrices of each element in the global coordinate, like Equation (32).

3. NONLINEAR EQUATION SOLVER

The incremental nonlinear static equation can be written in the following form:

$$\{F\} = [K]\{D\} \tag{33}$$

In this relation, {F} is the internal force vector, [K] is the nonlinear stiffness matrix in the global coordinate and {D} is the nodal displacement vector. In the normal way, there are three following ways for solving equation (33) and obtaining the static path of the geometric nonlinear problems: 1- Pure incremental method or linear incremental tactic, 2- Incremental-iterative procedure or nonlinear incremental approach, and 3- Direct strategy. It is worth mentioning that the linear incremental approach is easy to use, but it has a limited application. Because, in the structural analyses, which have large displacements and large rotations, may not be accurate [27].

The most effective techniques for the nonlinear structural analysis are the incremental-iterative methods. In these procedures, every loading step is consisted of two parts: incremental or predictor step and iterative or corrector step. At the first stage, by finding the incremental load factor, the primary approximation for displacement vector is obtained. At the second phase, the structural static path progresses through successive iterations. The Newton-Raphson method is a load control procedure which cannot trace the nonlinear region of a load-displacement curve beyond the load limit points [28]. In order to solve this problem, displacement control technique was introduced [29]. It should be noted that for structures with snap-back behavior, this strategy leads to inaccuracy responses.

To obtain a more general technique, researchers have proposed the arc-length approach for the nonlinear analysis of structures [30-32]. In the load control method, the load factor remains constant during iteration. Moreover, in the displacement control approach, the displacement factor is kept invariable. In contrast to these algorithms, when each iteration starts, in the arc-length process, the load factor is modified so that the solution follows some specified paths until reaching convergence. Due to existing variable load factor in analysis

procedure, an extra constraint equation in terms of the displacement is needed. It is worth emphasizing that various techniques have so far been suggested by the investigators to formulate the additional constraint equation. In the cylindrical arc-length method, Crisfield ignored the load component against the displacement component in constraint equation and suggested another approach, which is called Riks's improved technique [33].

This study uses the cylindrical arc-length technique with a variable stiffness matrix to solve elastic geometric nonlinear space truss problems. In the following subsections, the numerical procedure for this method is presented by using the update Lagrangian description in the higher-order analysis.

3.1 Cylindrical arc-length technique

The solution procedure of the cylindrical arc-length technique is presented in Fig. 2. Assuming the (n-1)th equilibrium point, analysis for attaining the (n)th point on the structural static path is carried out. At the beginning, in the predictor step, the amount of displacement is calculated by solving below equation:

$$K^{n-1}\Delta D_1^n = \Delta\lambda_1^n\, P \tag{34}$$

In the last relationship, K^{n-1} is the tangential stiffness matrix at the (n-1)th equilibrium point, and $\Delta\lambda$ is the incremental load factor. Employing equality (34), the coordinate of point 1 is obtained. Because this point is out of the structural static path, successive iterations are needed in the corrector step. In arc-length method, the distance of the all iteration points to previous equilibrium point is equal to the arc length which is kept fixed during an increment. This procedure is shown in Fig. 2.

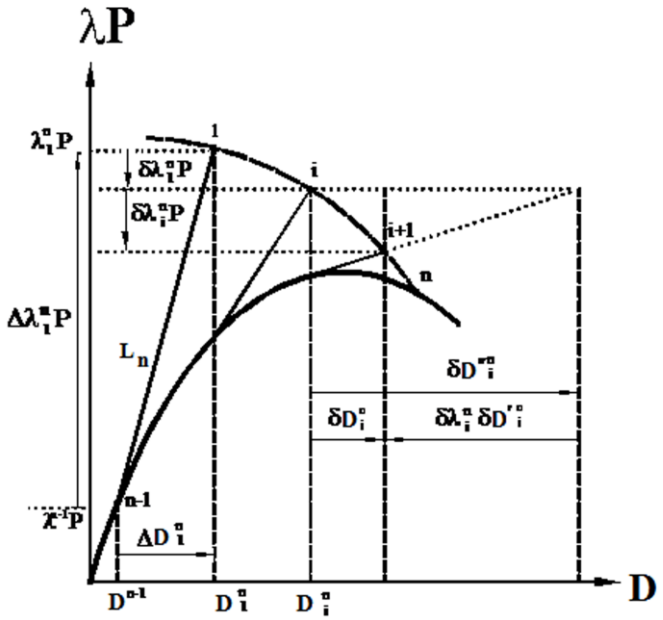

Figure 2. The structure of cylindrical arc-length method

Based on the Fig. 2, the following expression can be found for constraint equation:

$$\Delta D_i^{nT} \Delta D_i^n + \Psi^2 \Delta \lambda_i^n P^T \Delta \lambda_i^n P = {L_n}^2 \tag{35}$$

Where L_n is arc length at the (n)th increment, Ψ is a scaling parameter for loading terms. For the cylindrical arc-length, the scaling parameter Ψ is set to zero, and the constraint equation reads simply:

$$\Delta D_i^{nT} \Delta D_i^n = {L_n}^2 \tag{36}$$

In each iteration, the displacement has the next formula:

$$\delta D_i^n = \delta D_i''^n + \delta \lambda_i^n \delta D_i'^n \tag{37}$$

Here, $\delta D_i''^n$ and $\delta D_i'^n$ are displacements due to out of the balance force, R, and the external load, P, respectively. They can be calculated from the below equations:

$$K_i^n \delta D_i''^n = R_i^n \tag{38}$$

$$K_i^n \delta D_i'^n = P \tag{39}$$

On the other hand, the amount of the incremental load factor and incremental displacement are calculated by the help of following equations:

$$\Delta D_{i+1}^n = \Delta D_i^n + \delta D_i^n \tag{40}$$

$$\Delta \lambda_{i+1}^n = \Delta \lambda_i^n + \delta \lambda_i^n \tag{41}$$

According to the Fig. 2, the unbalanced load in the nth iteration (R_i^n) has the following amount:

$$R_i^n = \lambda_i^n P - F_i^n \tag{42}$$

In the former equality, F_i^n is the nodal load in the nth iteration. It should be noted that the system of equations (38) and (39) can be solved in terms of the quantities of unbalanced force, R, and the external load, P. Consequently, based on equation (37), in order to calculate δD_i^n, $\delta \lambda_i^n$ must be determined. By replacing equations (37-40) into relationship (36), the constraint equation can be expressed as below:

$$a(\delta\lambda_i^n)^2 + b(\delta\lambda_i^n) + c = 0 \tag{43}$$

Where:

$$a = (\delta D_i'^n)^T (\delta D_i'^n) \tag{44}$$

$$b = 2(\Delta D_i^n + \delta D_i''^n)^T (\delta D_i'^n) \tag{45}$$

$$c = 2(\Delta D_i^n + \delta D_i''^n)^T (\Delta D_i^n + \delta D_i''^n) - L_n{}^2 \tag{46}$$

Solving equation (43) leads to coming results for $\delta\lambda_i^n$:

$$\begin{cases} \delta\lambda_{i,1}^n \\ \delta\lambda_{i,1}^n \end{cases} = -\frac{b}{2a} \pm \sqrt{(\frac{b}{2a})^2 - \frac{c}{a}} \tag{47}$$

Which are real values if the following condition is satisfied:

$$\Delta = b^2 - 4ac \rangle 0 \tag{48}$$

One selects the root that corresponds to the point closest to the one obtained in the last iteration. This proximity can be assessed by the dot product:

$$(\Delta D_i^n + \delta D_i''^n + \delta\lambda_i^n \times \delta D_i'^n)^T \Delta D_i^n \tag{49}$$

This rule aims to prevent that the equilibrium path doubles back on itself. If the value of Δ in equation (48) becomes zero, only one root is real, and it can be used as the change of the load factor in the subsequent iteration. Furthermore, if Δ is negative, the two roots are virtual. Then, the arc length (L_n) should be given a reduction and begin again. In addition, the amount of the incremental load factor in predictor step in each loading step is calculated by the help of following equation:

$$\Delta\lambda_1^n = \pm \frac{L_n}{\sqrt{\delta u_1'^{nT} \delta u_1'^n}} \tag{50}$$

4. NUMERICAL EXAMPLES

To test the ability and accuracy of the proposed formulations, some nonlinear problems will be solved. The findings will be compared with the available responses, as well. It should be added that several space trusses have been analyzed by the authors' computer program, and a few of these structures will be presented in the subsequent subsections.

4.1 Four-member space truss

This structure, which is shown in Fig. 3, has four members. This symmetric single degree of freedom structure was utilized for checking several incremental-iterative methods [34]. Moreover, this three-dimensional truss was employed for studying the time step in dynamic relaxation strategy [35]. It is important to note that this structure exhibits a snap-through phenomenon.

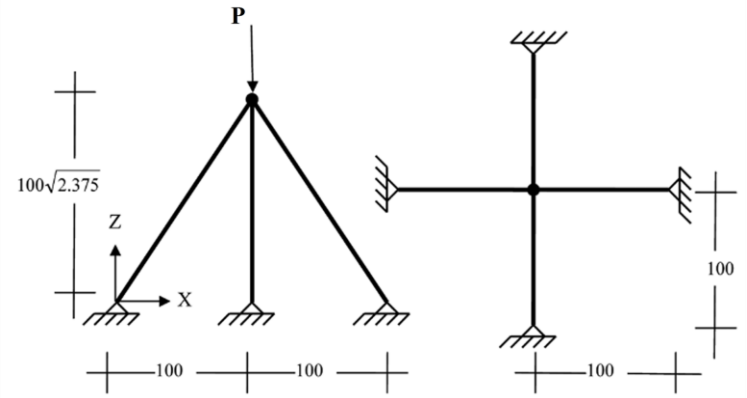

Figure 3. Four-member space truss (dimentions in mm)

The axial rigidity of each member is AE=10000 N [35]. A concentrated load of 1 N is applied at the top of the structure. Furthermore, it is assumed that the arc length is equal 5 in the loading steps.

A higher-order nonlinear analysis is performed on this structure by using the authors' stiffness matrix and also cylindrical arc-length method [33]. Fig. 4 shows the numerical results for this three-dimensional truss.

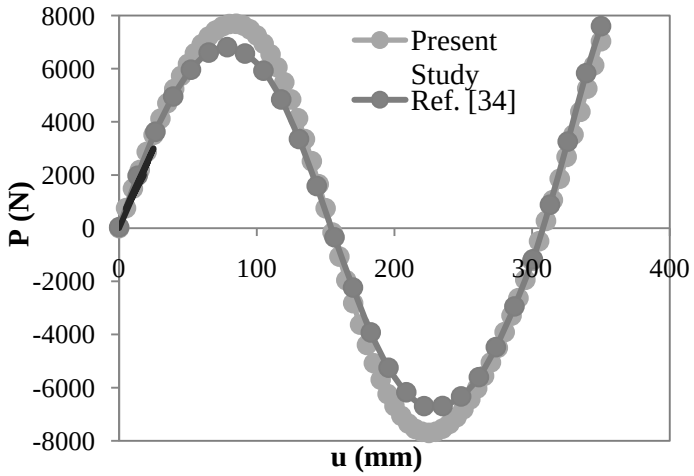

Figure 4. The load-displacement diagram for four-member space truss

As it is shown in the Fig. 4, the detected equilibrium path, which was found by using higher-order stiffness matrix, and the load-displacement curve, which was obtained by

Rezaiee-Pajand et al. [34], are the same. Moreover, the proposed method reaches to the load limit point after tracing the longer path in comparison with predecessors' tactic. Consequently, the new higher-order nonlinear technique is more accurate than the other strategy. In addition, the solution was quite consistent with the structural static path obtained by Rezaiee-Pajand et al. [35].

4.2 Star shape dome truss

Fig. 5 shows the geometry and loading of a short 24-member dome. The elasticity modulus of each member of the truss is $E=3\times10^5 N/cm^2$ and its cross section is $A=3.17cm^2$ [34]. A unit concentrated load is applied at the central node. Furthermore, the arc length in the loading steps is assumed 1.

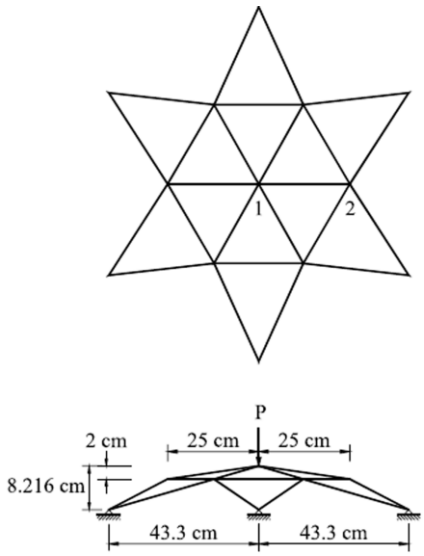

Figure 5. Star shape dome truss

The application of this example in the nonlinear analysis of space trusses is very common. This problem is utilized for examining three residual perimeter and area methods and cylindrical arc-length approach [36], surveying dynamic relaxation technique in the tracing of structures [37, 38]. The load-displacement curve of node 1 in the direction of load obtained by proposed higher-order nonlinear analysis and Rezaiee-Pajand et al. [34] are shown in Fig. 6. It is observed that the equilibrium path obtained with the suggested approach has very good agreement to the predecessors' results [34].

The static paths of the star truss at node 2 in the horizontal and vertical directions are also shown in Fig. 7. According to the load-displacement diagrams, the space truss exhibits snap-through in node 1, whereas node 2 shows snap-back behavior. According to the finding results, the higher-order stiffness matrix of the space truss completely covered the former investigators' load-displacement curves [18].

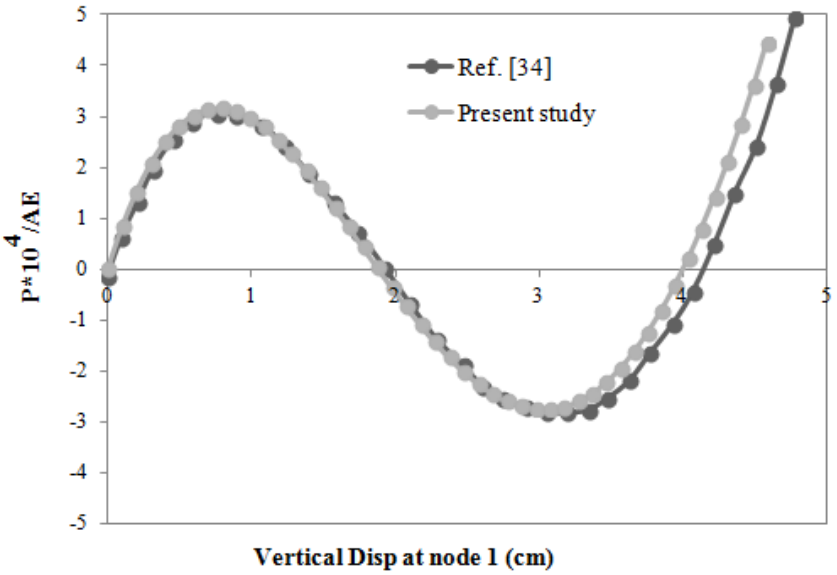

Figure 6. Load-displacement curves of the star shape dome truss for node 1

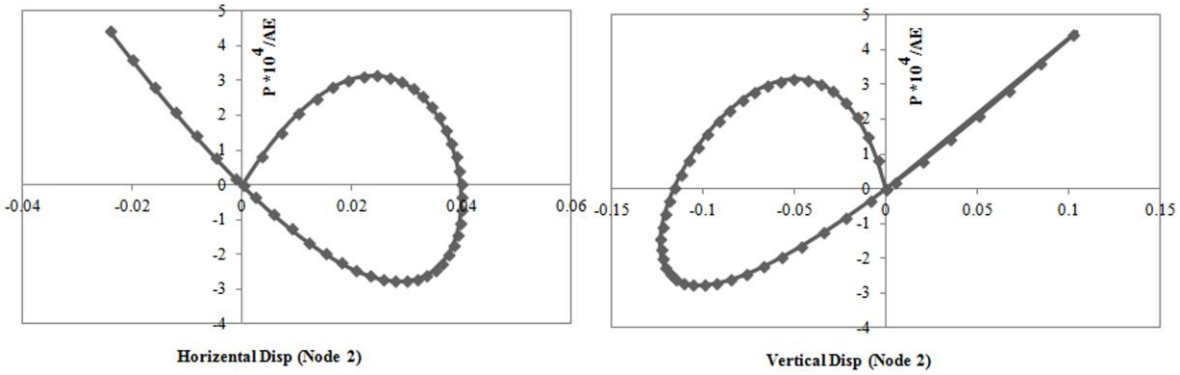

Figure 7. Load-displacement relation for Geometric shape dome truss at node 2: Horizontal direction; (b) Vertical direction

4.3 Geometric dome truss

The geometry and loading of a geometric dome truss with 156 members are shown in Fig. 8. All of members have equal cross sections. The elasticity modulus of the truss members is E=68950 N/mm^2 and their cross section is A=650 mm^2 [14, 40]. Moreover, the arc length in the loading steps is assumed 0.001. A concentrated force of 1 N is applied at the top of the truss. The elevation of this space truss is defined by the following equation:

$$x^2 + y^2 + (z + 7.2)^2 = 60.84 \tag{51}$$

Thus far the nonlinear analysis of this structure has been carried out by using various techniques, such as dynamic relaxation [39], and two-point method [40].

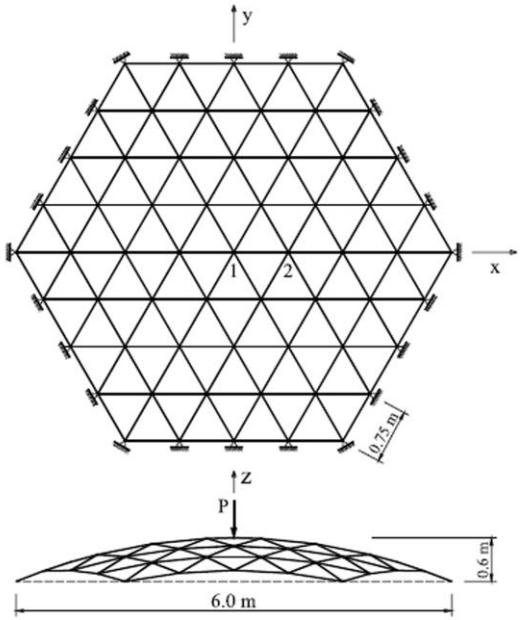

Figure 8. Geometric dome truss

Fig. 9 shows the comparison of the load-displacement curve of node 1 in the direction of the load obtained by present study and Thai and Kim [14]. It is observed that the curve generated by the proposed higher-order nonlinear analysis is in reasonable agreement with the predicted solution by Thai [14]. When the load reaches its maximum, P=3.23 kN, displacement is 13.32 cm, and a 1.54% difference occurs by comparing with Thai solution of P=3.18 kN.

The equilibrium paths of the dome truss at node 2 in the horizontal and vertical directions are also shown in Fig. 10. According to the obtained, by considering all the linear and nonlinear components of the strain vector, the new tactic can trace the structural path more accurately [14].

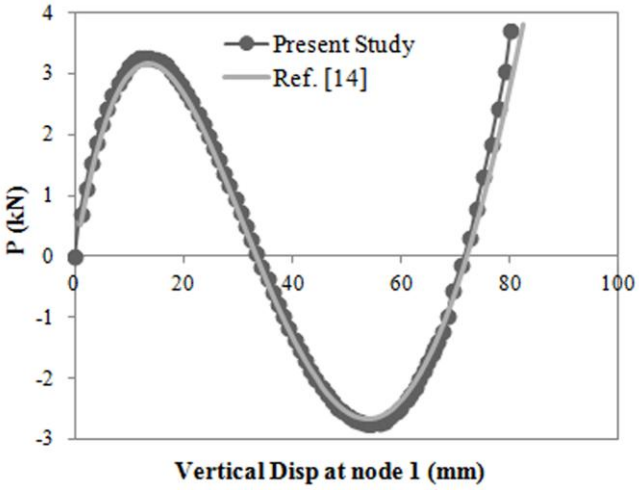

Figure 9. Load-displacement curves of Geometric dome truss at node 1

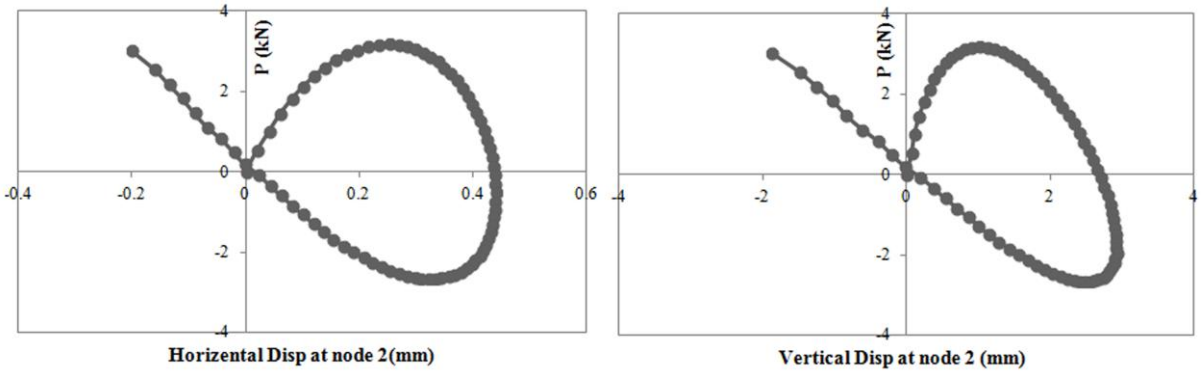

Figure 10. Load-displacement relation for Geometric shape dome truss at node 2: (a) Horizontal direction; (b) Vertical direction

5. CONCLUSION

Some of the three-dimensional trusses experience large displacements under loads. In order to analyze these structures, a capable tangent stiffness matrix is required. A geometric nonlinear formulation was proposed for the prediction of the static equilibrium paths of the space trusses. In this article, all parts of the strain-displacement relationships were used to establish a robust tangent stiffness matrix. Due to elastic behavior of the truss, the minimization of total potential energy and also the relation of virtual work were utilized in this study. After describing the formulations in detail, the ability of the suggested scheme was studied by some sample examples. In fact, a lot of numerical tests were performed to show the ability of the authors' strategy. Due to volume limitation, a few of the solved problems were given in this paper. All the obtained numerical results and the solutions of former researchers were equivalent. Including the second-order strain terms affected the calculated unbalanced force vector as well as the element tangent stiffness. This was the reason that the authors' technique had better convergence speed of the solution process, and was more accurate in comparison with the previously presented methods.

APPENDIX

The elastic and geometric stiffness matrices, and also all parts of the higher-order stiffness matrices for the space truss are given in the following lines:

$$[K_0] = \frac{EA}{L}\begin{bmatrix} 1 & 0 & 0 & -1 & 0 & 0 \\ 0 & 0 & 0 & 0 & 0 & 0 \\ 0 & 0 & 0 & 0 & 0 & 0 \\ -1 & 0 & 0 & 1 & 0 & 0 \\ 0 & 0 & 0 & 0 & 0 & 0 \\ 0 & 0 & 0 & 0 & 0 & 0 \end{bmatrix} \tag{52}$$

$$[K_P] = \frac{P}{L}\begin{bmatrix} 1 & 0 & 0 & -1 & 0 & 0 \\ 0 & 1 & 0 & 0 & -1 & 0 \\ 0 & 0 & 1 & 0 & 0 & -1 \\ -1 & 0 & 0 & 1 & 0 & 0 \\ 0 & -1 & 0 & 0 & 1 & 0 \\ 0 & 0 & -1 & 0 & 0 & 1 \end{bmatrix} \tag{53}$$

$$[K_1] = \frac{EA}{2L^2}\begin{bmatrix} \Delta u & \Delta v & \Delta w & -\Delta u & -\Delta v & -\Delta w \\ 0 & 0 & 0 & 0 & 0 & 0 \\ 0 & 0 & 0 & 0 & 0 & 0 \\ -\Delta u & -\Delta v & -\Delta w & \Delta u & \Delta v & \Delta w \\ 0 & 0 & 0 & 0 & 0 & 0 \\ 0 & 0 & 0 & 0 & 0 & 0 \end{bmatrix} \tag{54}$$

$$[K_2] = \frac{EA}{L^2}\begin{bmatrix} \Delta u & 0 & 0 & -\Delta u & 0 & 0 \\ \Delta v & 0 & 0 & -\Delta v & 0 & 0 \\ \Delta w & 0 & 0 & -\Delta w & 0 & 0 \\ -\Delta u & 0 & 0 & \Delta u & 0 & 0 \\ -\Delta v & 0 & 0 & \Delta v & 0 & 0 \\ -\Delta w & 0 & 0 & \Delta w & 0 & 0 \end{bmatrix} \tag{55}$$

$$[K_3] = \frac{EA}{2L^3}\begin{bmatrix} \Delta u^2 & \Delta u\Delta v & \Delta u\Delta w & -\Delta u^2 & -\Delta u\Delta v & -\Delta u\Delta w \\ \Delta u\Delta v & \Delta v^2 & \Delta v\Delta w & -\Delta u\Delta v & -\Delta v^2 & -\Delta v\Delta w \\ \Delta u\Delta w & \Delta v\Delta w & \Delta w^2 & -\Delta u\Delta w & -\Delta v\Delta w & -\Delta w^2 \\ -\Delta u^2 & -\Delta u\Delta v & -\Delta u\Delta w & \Delta u^2 & \Delta u\Delta v & \Delta u\Delta w \\ -\Delta u\Delta v & -\Delta v^2 & -\Delta v\Delta w & \Delta u\Delta v & \Delta v^2 & \Delta v\Delta w \\ -\Delta u\Delta w & -\Delta v\Delta w & -\Delta w^2 & \Delta u\Delta w & \Delta v\Delta w & \Delta w^2 \end{bmatrix} \tag{56}$$

In these relationships, the below parameters are used:

$$\Delta u = u_2 - u_1$$
$$\Delta v = v_2 - v_1 \quad (57)$$
$$\Delta w = w_2 - w_1$$

REFERENCES

1. Jagannathan DS, Epstein HI, Christiano P. Nonlinear analysis of reticulated space trusses, *Journal of Structural Engineering, ASCE*, No. 12, **101**(1975) 2641-58.
2. Rothert H, Dickel T, Renner D. Snap-though buckling of reticulated space trusses, *Journal of the Structural Division, ASCE*, No. 1, **107**(1981) 129-43.
3. Holzer SM, Plaut RM, Somers AE. Jr, White WS. Ill. Stability of lattice structure under combined loads, *Journal of the Structural Division, ASCE*, No. 2, **106**(1980) 289-305.
4. Papadrakakis M. Post-buckling analysis of spatial structures by vector iteration method, *Computer and Structures*, Nos. 5-6, **14**(1981) 393-402.
5. Papadrakakis M. Post-buckling analysis of trusses, *Journal of Structural Engineering (ASCE)*, No. 9, **109**(1983) 2129-47.
6. Pecknold DA, Ghaboussi J, Healey TJ. Snap-through and bifurcation in a simple structure, *Journal of Engineering Mechanics (ASCE)*, No. 7, **111**(1985) 909-22.
7. Kondoh K, Atluri SN. Influence of the local buckling on global stability: simplified, large deformation, post-buckling analysis of plane trusses, *Computer and Structures*, No. 4, **21**(1985) 613-27.
8. Hill CD, Blandford GE, Wang ST. Post-buckling analysis of steel space trusses, *Journal of Structural Engineering, (ASCE)*, No. 4, **115**(1989) 900-19.
9. Ramesh G, Krishnamoorthy CS. Inelastic post-buckling analysis of truss structures by dynamic relaxation method, *International Journal for Numerical Methods in Engineering*, No. 21, **37**(1994) 3633-57.
10. Blandford G. Large deformation analysis of inelastic space truss structures, *Journal of Structural Engineering, ASCE*, No. 4, **122**(1996) 407-15.
11. Blandford G. Progressive failure analysis of inelastic space truss structures, *Computer and Structures*, No. 5, **58**(1996) 981-90.
12. Toklu YC. Nonlinear analysis of trusses through energy minimization, *Computer and Structures*, Nos. 20-21, **82**(2004) 1581-9.
13. Saffari H, Fadaee MJ, Tabatabaei R. Nonlinear analysis of space trusses using modified normal flow algorithm, *Journal of Structural Engineering, (ASCE)*, No. 6, **134**(2008) 998-1005.

14. Thai HT, Kim SE. Large deflection inelastic analysis of space trusses using generalized displacement control method, *Journal of Constructional Steel Research*, Nos. 10-11, **65**(2009) 1987-94.
15. Zhou Z, Meng SP, Wu J. Stability analysis of prestresses space truss structures based on the imperfect truss element, *International Journal of Steel Structures*, No. 3, **9**(2009) 253-60.
16. Torkamani MAM, Shieh JH. Higher-order stiffness matrices in nonlinear finite element analysis of plane truss structures, *Engineering Structures*, No. 12, **33**(2011) 3516-26.
17. Mondkar DP, Powell GH. Finite element analysis of non-linear static and dynamic response, *International Journal of Steel Structures*, No. 3, **11**(1977) 499-520.
18. Meek JL, Tan HS. Geometrically nonlinear analysis of space frames by an incremental iterative technique, *Computer Methods in Applied Mechanics and Engineering*, No. 3, **47**(1984) 261-82.
19. Crisfield MA. A consistent corotational formulation for nonlinear three dimensional beam-elements, *Computer Methods in Applied Mechanics and Engineering*, No. 2, **81**(1990) 131-50.
20. Torkamani MAM, Sonmez M. Inelastic large deflection modeling of beam columns, *Journal of Structural Engineering, (ASCE)*, No. 8, **127**(2001) 876-87.
21. Yang YB, Lin SP, Wang CM. Rigid element approach for deriving the geometric stiffness of curved beams for use in buckling analysis, *Journal of Structural Engineering, ASCE*, No. 12, **133**(2007) 1762-71.
22. Yang YB, Kuo SR. Theory & analysis of nonlinear framed structures, Singapore, 1994.
23. Bazeley GP, Cheung YK, Irons BM, Zienkiewics OC. Triangular elements in plate bending-conforming and nonconforming solutions, *First Conference on Matrix Methods in Structural Mechanics*, Ohio, 1965, pp. 547-576.
24. Taylor RL, Simo JC, Zienkiewics OC, Chan ACH. The patch test - A condition for assessing FEM convergence, *International Journal for Numerical Methods in Engineering*, No. 1, **22**(1986) 39-62.
25. Cook RD, Malkus DS, Plesha ME. *Concepts and Applications of Finite Element Analysis*, 3rd edn, John Wiley, New York, NY, 1989.
26. Yang YB, Chou JH, Leu LJ. Rigid body considerations for nonlinear finite element analysis, *International Journal for Numerical Methods in Engineering*, No. 8, **33**(1992) 1597-1610.
27. Chajes A, Churchill JE. Nonlinear frame analysis by finite element methods, *Journal of Structural Engineering, (ASCE)*, No. 6, **113**(1987) 1221-35.
28. Torkamani M, Sonmez M. Solution techniques for nonlinear equilibrium equations, *Structures Congress, ASCE*, (2008) 1-17.

29. Zinkiewicz OC. Incremental displacement in non-Linear analysis, *International Journal for Numerical Methods in Engineering*, No. 4, **3**(1971) 587-92.
30. Wempner GA. Discrete approximation related to nonlinear theories of solids, *International Journal of Solids and Structures*, No. 11, **7**(1971) 1581-99.
31. Riks E. The application of Newton's method to the problem of elastic stability, *Journal of Applied Mechanics*, **39**(1972) 1060-5.
32. Riks E. An incremental approach to the solution of snapping and buckling problems, *International Journal of Solids and Structures*, No. 7, **15**(1979) 529-51.
33. Crisfield MA. A fast incremental/iterative solution procedure that handles snap-through, *Computer and Structures*, Nos. 1-3, **13**(1981) 55-62.
34. Rezaiee-Pajand M, Tatar M, Moghaddasie B. Some geometrical bases for incremental-iterative methods, *International Journal of Engineering, Transactions B: Applications*, No. 3, **22**(2009) 245-56.
35. Rezaiee-Pajand M, Kadkhodayan M, Alamatian J. Timestep selection for dynamic relaxation method, *Mechanics Based Design of Structures and Machines*, No. 1, **40**(2012) 42-72.
36. Rezaiee-Pajand M, Naserian R. Using residual areas for geometrically nonlinear structural analysis, Ocean Engineering, No. 105, 1(2015) 327-35.
37. Rezaiee-Pajand M, Sarafrazi SR, Rezaiee H. Efficiency of Dynamic relaxation methods in nonlinear analysis of truss and frame structures, Computers and Structures, Nos. 112-113, (2012) 295-10.
38. Rezaiee-Pajand M, Alamatian J. Automatic DR structural analysis of snap-through and snap-back using optimized load increments, *Journal of Structural Engineering, ASCE*, No. 1, **137**(2011) 109-16.
39. Rezaiee-Pajand M, Sarafrazi SR. Nonlinear dynamic structural analysis using dynamic relaxation with zero damping, *Computer and Structures*, Nos. 13-14, **89**(2011) 1274-85.
40. Saffari H, Mansouri I. Non-linear analysis of structures using two-point method, *International Journal of Non-Linear Mechanics*, No. 6, **46**(2011) 834-40.